Optimal content of bio-fibers in structural ice

Materials and Structures (2024) 57:177
https://doi.org/10.1617/s11527-024-02455-2

ORIGINAL ARTICLE

Optimal content of bio-fibers in structural ice

Alessandro P. Fantilli · Barbara Frigo · Farmehr M. Dehkordi

Received: 23 March 2024 / Accepted: 30 August 2024 / Published online: 10 September 2024

Abstract The use of ice as structural material has two main concerns: the low strength and the brittle failure of the structures. With the aim of finding a solution to these problems, an experimental campaign, performed on fiber-reinforced ice (FRI) samples, made with plain water and bio-fibers, is presented in this paper. In total, 12 ice prisms were cast at − 18 °C with a different content of fibers, and then tested in three-point bending and uniaxial compression. Test results indicate that the presence of a reinforcement increases both flexural and compressive strength with respect to plain ice. Moreover, FRI is a tougher material, as multiple cracking and deflection hardening behavior can be observed in the flexural tests. However, the mechanical performances of plain ice are not always enhanced by the fiber-reinforcement. Therefore, an empirical model, capable of predicting the optimal content of bio-fibers, is also proposed.

Keywords Two stage casting · Three-point bending test · Uniaxial compression test · Post-cracking behavior

List of symbols

a	Coefficient in Eq. (3)
B	Width of beam cross-section
f_c	Compressive strength of ice
$f_{f,u}$	Ultimate flexural strength (when $P = P_u$ in Eq. (4)
$f_{f,cr}$	Flexural strength at cracking (when $P = P_{cr}$ in Eq. (4))
H	Height of the beam cross-section
L	Length of the beam span
P	Applied load
P_c	Maximum load of compression test
P_{cr}	Applied load at first cracking in bending
P_u	Maximum load of bending test
QF	Quantity of fibers
R^2	Coefficient of determination
W	Work (or the energy) released during the deflection-hardening
wt	Weight of the samples
α, β, γ	Coefficients in Eq. (4)
Δ	Difference between the deflection measured at P_u and that in correspondence of P_{cr}
η	Mid-span deflection of the beam

A. P. Fantilli (✉) · B. Frigo · F. M. Dehkordi
Department of Structural, Building, and Geotechnical Engineering-DISEG, Politecnico di Torino, Corso Duca degli Abruzzi 24, 10129 Turin, Italy
e-mail: alessandro.fantilli@polito.it

B. Frigo
e-mail: barbara.frigo@polito.it

F. M. Dehkordi
e-mail: farmehr.mohammadpour@polito.it

1 Introduction

The development of scientific research to improve material performances and technologies is an important task, especially in cold regions, where ice is sometimes a construction material [1]. Ice structures, like frozen hotels, igloos, and winter constructions, could not appear innovative. Indeed, studies on the use of ice as construction material have been performed since ancient times, especially in polar environment [2]. However, from a green engineering perspective, ice is a highly convenient and sustainable building material, because it is not only 'self-created', but it can be easily removed at the end of the use without any problem for the environment.

Recently, new applications in zones with all-year-low temperatures have been explored [3]. They have focused on the use in low-tech structures, such as ice roads, ice dams, and ice domes, all of which have proven to be energy-efficient and altogether sustainable. For instance, the Ice Hotel in Sweden, which is reconstructed annually using ice blocks from the nearby Torne River, is a well-known example of the use of ice as a building material in modern construction [4]. Similarly, the use of reinforced ice composites in temporary winter roads across Canada and Russia has shown the potential of ice as a reliable material under extreme conditions [5].

These examples underscore the ongoing relevance and innovation in using ice as a structural material in cold regions, especially when ice is combined with other materials (e.g., sawdust) to form the so-called Pykrete [6]. Table 1 presents a selection of historical applications of different ice composites in structural elements.

Despite the several advantages, ice constructions arise lots of concerns, due to the weak strength and brittle failure of the structural elements, which limits the applications of ice in the construction industry. For these reasons, researchers tried to reinforce plain ice in two ways. Firstly, macro elements, which can be embedded within the ice element in order to resist to the tensile stresses, were added. The sizes of such macroscopic reinforcement, like tree trunks, steel rebar, and geogrid [9], are much larger than ice grains [10].

Secondly, ice performances were enhanced by adding a strengthening material of the same size of the ice grain (small or microscopic). This is the case of sawdust in Pykrete, which can be considered as a reinforcement uniformly blended within water [11]. After freezing, the size of reinforcement is comparable with that of the microstructural scale of ice, and create an essentially isotropic material [12]. Wood dowels and cut lumber are some examples of micro-additions that improve the mechanical performances of ice [13].

Recently, the addition of fibers in the so-called fiber-reinforced ice (FRI) has attracted the attention of researchers and practitioners. Indeed, the presence of fibers significantly minimizes the stress concentration at the crack tip of the process zone, preventing the rapid crack growth and greatly improving the toughness with respect to plain ice [14]. However, some of the fibers used in the past cannot be considered an option for the current requirements, as the final product must be environmental-friendly. Moreover, FRI has to guarantee acceptable strength both in tension and in compression, whereas, in previous studies, researchers generally performed compression tests on

Table 1 Historical examples of ice structures

Period	Material or Method	Structure	References
Ancient	Lichen + Ice	Igloo	[7]
Second world war	Logs, branches, and twigs + Ice	Ice roads and ferries	[7]
	Wood pulp (pykrete) + Ice	Aircraft carrier	[7]
Cold war	Fiberglass + Ice	Ice airstrip	[8]
	Sawdust (pykrete) + Ice	Ice roads crossing swamps	[8]
	Wooden covering + Ice	Ice working space	[8]
Nowadays	Geo-nets from fiberglass + Ice	Ice roads	[8]
	Cytotropic gel formation + Ice	watertight elements	[8]
	Pykrete + Ice	Ice dome	[8]

cylindrical samples, without considering the effect of fiber content on the flexural strength [15, 16].

Thus, with the aim of expanding the knowledge of the mechanical behavior of FRI, and exploring the use of large volumes of bio-fibers, both bending and compression tests have been performed and described in the following sections. The goal is to tailor new ice-based materials in which flexural and compression strengths are increased by adding bio-fibers. As strength is an important parameter to design safe ice structures, the authors believe that the results of this research project can be useful to build more reliable and sustainable ice-constructions in cold regions.

2 Experimental investigation

2.1 Materials and specimen preparation

Pine needles were used as reinforcement of ice elements (Fig. 1). These bio-fibers can be found on evergreen trees (even if a pine tree is not necessarily an evergreen), on over 110 species of "*Pinus genus*" throughout the world. They are native to all the continents and are predominant in cold climates of Europe, Asia, North America, and various island countries [17].

A series of measurements, including length and diameter of the fibers, was conducted in the laboratory of Politecnico di Torino (Italy) using a caliper with an accuracy of 0.01 mm. Based on approximately 300 measurements, the average values of diameter, length, and aspect ratio (i.e., the ratio between length and diameter) of pine needles were equal to 1.26 mm, 91.4 mm, and 73.37, respectively. The statistical distributions of these parameters are also illustrated in Fig. 2.

Fig. 1 Pine needle used as fiber-reinforcement for ice

To cast FRI specimens, two-steps casting procedure was adopted. Firstly, pine needles were placed in the polystyrene molds, as shown in Fig. 3a. In each mold, three specimens having the dimensions of $40 \times 40 \times 160$ mm^3 were cast, similarly to the preparation of cement-based mortars [18]. Afterwards, the mold was filled with tap water (Fig. 3b), and both fibers and water remained at environmental conditions. After one day, the mold was filled again with water (some of the water evaporated and some was absorbed by fibers) and left in the freezer at—18 °C for 48 h. After de-molding, the samples were kept in the freezer to avoid melting at environmental temperature.

Four series of three specimens were cast by adopting this procedure and by changing the quantity of fibers QF:

- QF = 0 g/dm.^{3} in plain ice (PI)
- QF = 39 g/dm.^{3} in the first fiber-reinforced ice (FRI-1)
- QF = 56 g/dm.^{3} in the second fiber-reinforced ice (FRI-2)
- QF = 78 g/dm^3 in the third fiber-reinforced ice (FRI-3).

In total 12 specimens were prepared and tested according to the procedure suggested by UNI EN 196–1 [19] for cement-based mortars.

2.2 Testing procedure

Both flexural and compressive tests were carried out on the same specimen. In particular, all the samples were tested in three-point bending (see Fig. 4a) by applying the load *P,* in the midsection of the ice prisms, through a loading machine (having a capacity of 50 kN). Tests were performed by driving the displacement of the loading cell, whose stroke moved at a velocity of 0.04 mm per minute. The applied load P and the midspan deflection η of the beam were measured during the tests, till the complete failure of the specimen. This process generally

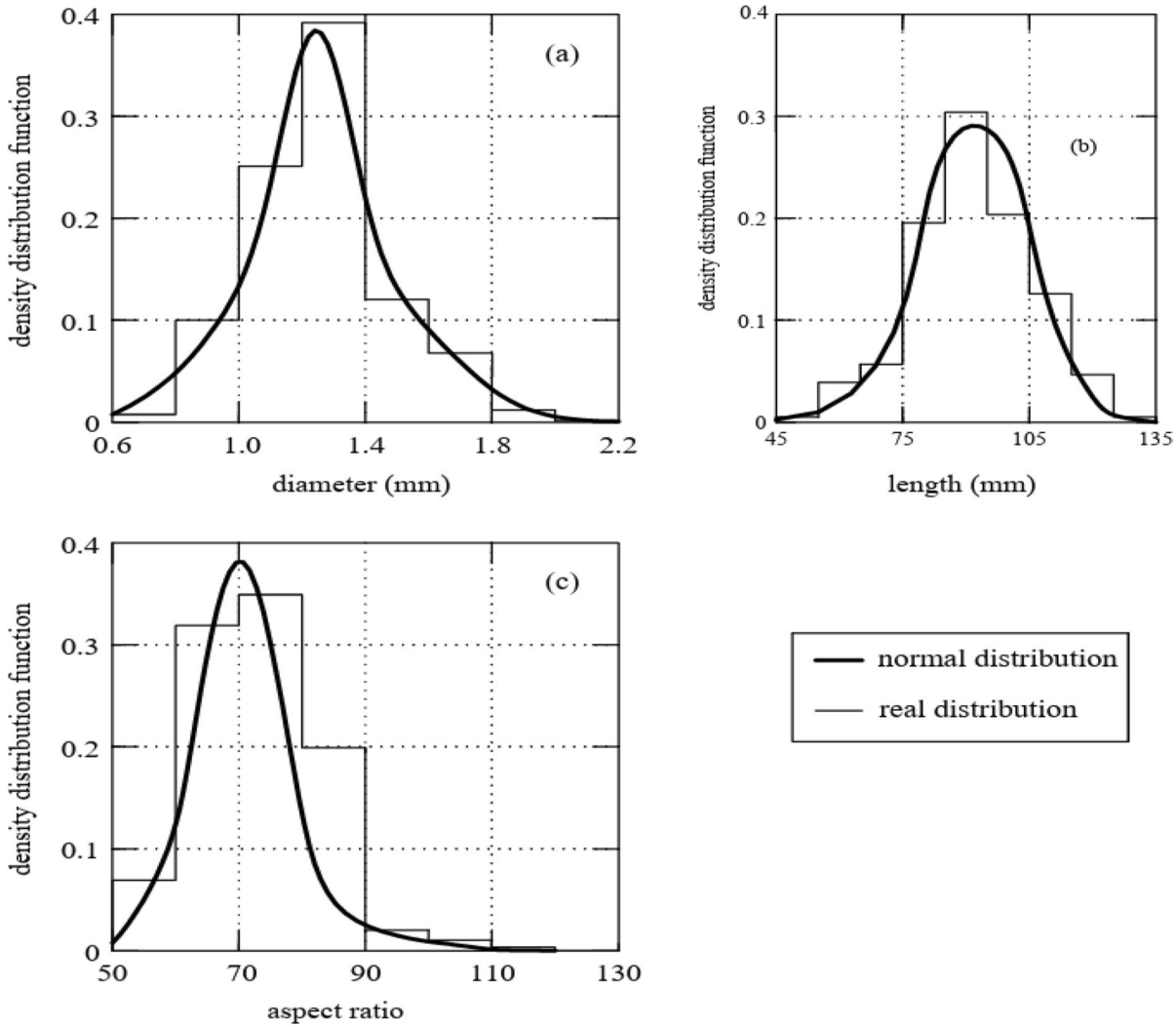

Fig. 2 Geometrical properties of pine needles used in this project: (**a**) statistical distribution of fiber diameter; (**b**) statistical distribution of fiber length; and (**c**) statistical distribution of fiber aspect ratio

broke the specimens into two halves, which were subsequently tested in compression (Fig. 4b).

In the uniaxial compression test, the load P was applied on a loading area of 40×40 mm^2, using a device with platens having a thickness of 10 mm. The compressive force P was gradually raised at a rate of 200 N per second up to the failure. In both flexural and compression tests, to avoid the problem of ice melting around the supports, a set of cooled rubber pieces were located on the points where specimens and loading machine were in contact.

3 Tests results

The weight (wt) of each specimen was measured with an accuracy of 0.01 N, whereas the width (B), height (H), and length (L) of the ice prisms were measured with a caliper having an accuracy of 0.01 mm. All the measurements are reported in Table 2. With these data, it was possible to measure the density of all the series investigated in this research project. The results, as reported in the last columns of Table 2, show that the density of the prisms did not change

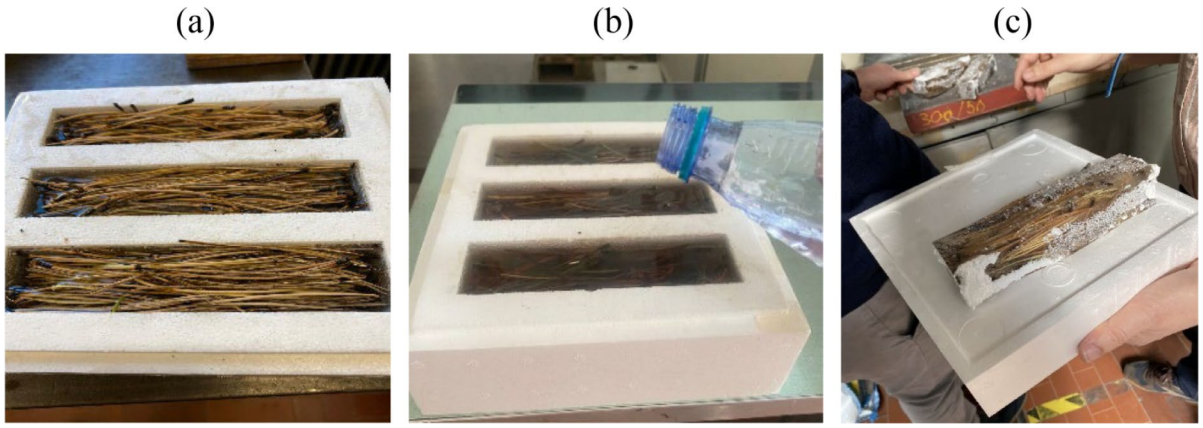

Fig. 3 Procedure used to prepare FRI specimens: (**a**) placing fibers in the molds; (**b**) pouring the water in the molds; (**c**) demolding the samples

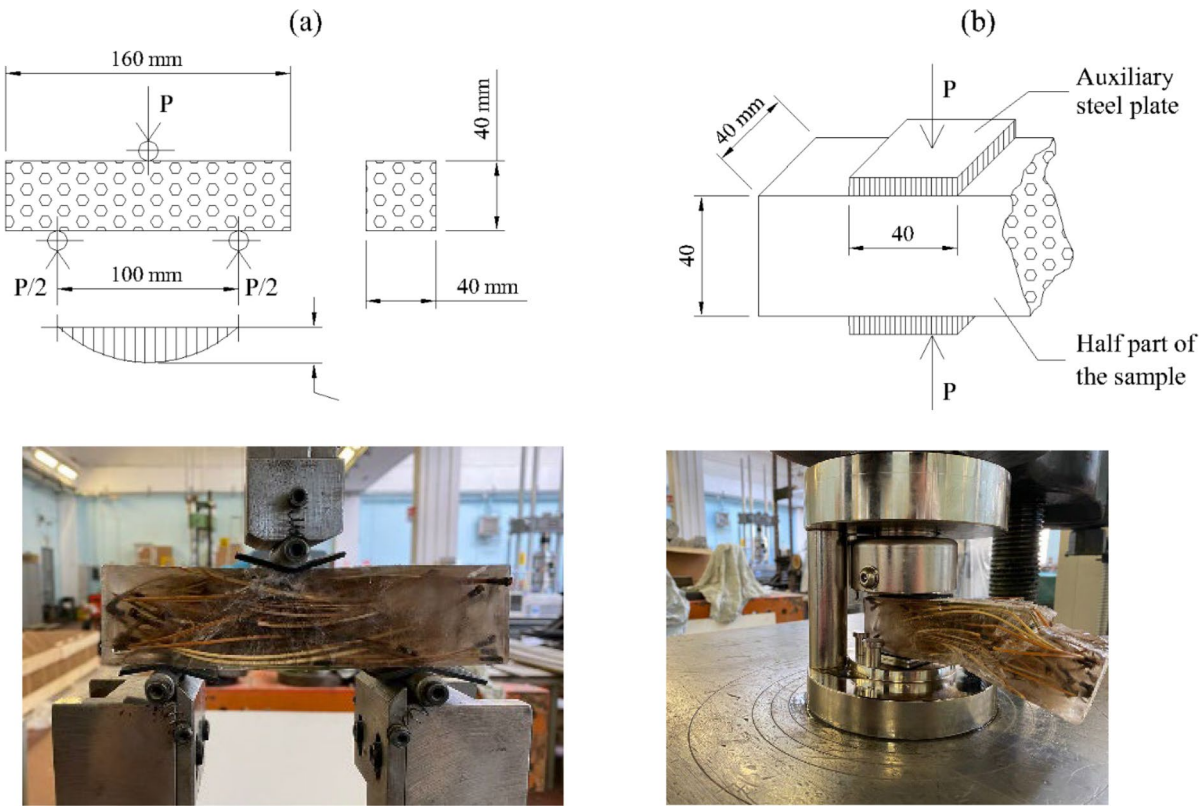

Fig. 4 Mechanical performances of fiber-reinforced ice: (**a**) three-point bending test; and (**b**) compression test

Table 2 Size and density of the ice samples

	QF (g/dm^3)	Sample	*B* (mm)	*H* (mm)	*L* (mm)	Before bending test		After bending test	
						wt (N)	Density (kg/m^3)	*wt* (N)	Density (kg/m^3)
PI	0	1	41.02	39.97	159.53	2.28	870	2.28	870
		2	42.53	39.75	159.17	2.35	870	2.34	870
		3	43.18	40.17	159.12	2.45	890	2.44	890
FRI-1	39	1	38.17	40.25	159.57	2.16	880	2.16	880
		2	38.57	40.65	159.67	2.25	900	2.25	900
		3	39.75	41.3	159.76	2.16	820	2.16	820
FRI-2	56	1	39.11	41.43	160.14	2.33	900	2.33	900
		2	41.45	40.53	160.11	2.34	870	2.34	870
		3	43.05	40.81	160.19	2.34	830	2.34	830
FRI-3	78	1	43.02	41.4	160.4	2.37	830	2.37	830
		2	43.01	40.78	160.34	2.4	850	2.38	850
		3	41.85	40.85	159.43	2.34	860	2.34	860

significantly in presence of fibers. In particular, the average value of 870 kg/m^3 was similar to that measured in other experimental campaigns [6]. As the tests were performed at environmental temperature, the weight and the density were measured before and after the bending test. As shown in Table 2, there was not a significant loss of weight (due to the melting of ice) during the test.

By means of the three-point bending tests, the load *P* versus the midspan deflection η diagrams were obtained for all the specimens. They are illustrated in Fig. 5, where they are grouped according to the content of fibers. The general ascending branch of all the *P*-η diagrams of FRI is illustrated in the ideal diagram of Fig. 6a. In this stage, more

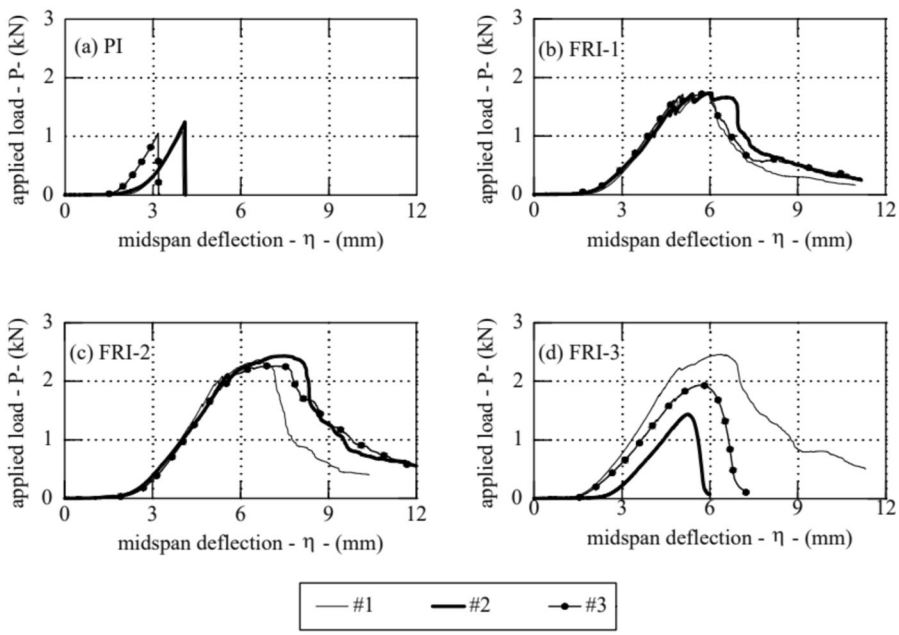

Fig. 5 Load-midspan deflection diagrams measured with the three-point bending tests

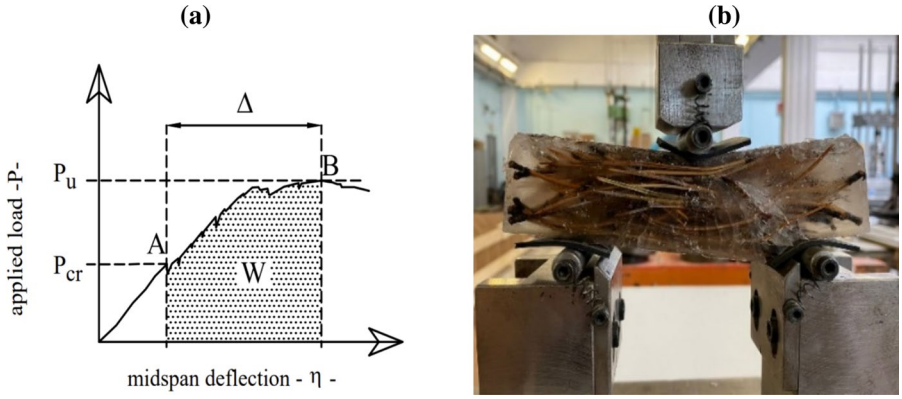

Fig. 6 Results of three-point bending tests: (**a**) ideal *P*-η curve in the rising branch. (**b**) multiple cracking in the fiber-reinforced ice samples

Table 3 Results of the three–point bending and compression tests

	QF (g/dm^3)	Sample	P_u (N)	P_{cr} (N)	Δ (mm)	P_c (N)
PI	0	1	1089		0	3654.14
		2	1236		0	2595.43
		3	1044		0	3017.55
FRI-1	39	1	1719	1617	1.025	5305.73
		2	1725	1488	1.242	5042.40
		3	1724	1600	1.060	3972.87
FRI-2	56	1	2365	2006	1.429	4681.68
		2	2423	2101	1.907	4295.47
		3	2251	1950	1.487	4880.62
FRI-3	78	1	2454	2220	1.401	4397.93
		2	1435	1272	0.847	3736.93
		3	1926	1692	0.917	3593.79

than one crack grows and a deflection hardening branch appears because of the fiber-reinforcement. Afterwards, a softening tail was observed, and loads decreased with the increment of the deflection. In this figure, two loads are important: P_{cr} at the first crack initiation (Point A in Fig. 6a), and P_u at the maximum load (point B in Fig. 6a). The values of these loads are indicated in Table 3. In the same table, the distance Δ between P_u and P_{cr} (see Fig. 6a), measured as the difference of the displacements η, is also reported. Finally, Table 3 also contains the maximum load P_c measured during the compression tests (Fig. 4b).

4 Analysis of results and discussion

Regarding the three-point bending tests, under the hypothesis of linear elastic behavior of materials and uncracked cross sections, the flexural stress can be calculated as follows:

$$f = P \cdot \frac{3 \cdot L}{2 \cdot B \cdot H^2} \tag{1}$$

Depending on the values of P (i.e., P_{cr} or P_u), it is possible to calculate the flexural strength at cracking $f_{f,cr}$, and the ultimate flexural strength $f_{f,u}$ by means of Eq. (1). The values of these strengths are reported in Table 4. In addition, the average values of $f_{f,cr}$ and $f_{f,u}$, measured for each type of FRI, are illustrated in the histograms of Fig. 7a and

Table 4 Mechanical properties measured in flexural and compression tests

	QF (g/dm^3)	Sample	$f_{f,cr}$ (MPa)	$f_{f,u}$ (MPa)	f_c (MPa)	W (kN·mm)
PI	0	1	2.49		2.28	0.0
		2	2.76		1.62	0.0
		3	2.25		1.89	0.0
FRI-1	39	1	3.84	4.09	3.32	1.7090
		2	3.29	3.82	3.15	1.9967
		3	3.57	3.85	2.48	1.7618
FRI-2	56	1	4.48	5.28	2.93	3.1243
		2	4.63	5.33	2.68	4.3130
		3	4.08	4.71	3.05	3.1239
FRI-3	78	1	4.51	4.99	2.75	3.2746
		2	2.52	2.85	2.34	1.1455
		3	3.63	4.13	2.25	1.6583

Fig. 7b, respectively. Obviously, $f_{f,cr}=f_{f,u}$ in the case of plain ice (PI), as $P_{cr}=P_u$ in absence of bio-fibers.

According to the ascending branch of the P-η diagram presented in Fig. 6a, it is possible to also calculate the work (or the energy) W associated with multiple cracking during a deflection-hardening stage:

$$W = \Delta \cdot \frac{P_{cr}+P_u}{2} \tag{2}$$

The values of W are presented in Table 4, whereas the average values of energy associated to the strain hardening stage of each FRI are reported in Fig. 7c. Finally, the values of compressive strength, evaluated by dividing P_c (in Table 3) by the loading area 40×40 mm^2, are also reported in Table 4 and Fig. 7d. In the latter Figure, the average values of compressive strength of each type of FRI are compared.

As two values of flexural strength (i.e., at cracking $f_{f,cr}$ and failure $f_{f,u}$) are herein considered, Fig. 8a, b shows the correlation between $f_{f,cr}$ and f_c, and between $f_{f,u}$ and f_c, respectively. The values of both these flexural strengths tend to linearly increase with the increment of compressive strength, as it generally occurs in brittle materials like concrete [20]. In particular, the following linear relationship, obtained with the least square approximation of the experimental data, can be used to predict the flexural strengths when compressive strength is known:

$$f_f = a \cdot f_c \tag{3}$$

where the values of coefficient a, reported in Table 5, depends on the type of flexural strength. To have an indicator of the reliability of these interpolations, the values of the coefficient of determination R^2 is also included in the same Table. Equation (3) can be effectively used to design of FRI structures in bending [21], when only compressive strength is known.

Test results can also be reported as a function of the quantity of fibers (QF). However, as shown in Fig. 7 the increment of QF does not necessarily produce an increment of all the mechanical performances. In fact, the values of strength and energy are not monotonic functions of QF. As depicted in the diagrams of Fig. 9, where the values of $f_{f,cr}$, $f_{f,u}$, W, and f_c are reported as a function of QF, a regression analysis, based on the least square approximation of the experimental data, is leading to the derivation of the following quadric function:

$$\text{Mechanical performance} = (\alpha \cdot QF^2) + (\beta \cdot QF) + \gamma \tag{4}$$

where the coefficients α, β, and γ depend on the type of mechanical performance, as reported in Table 6.

According to the experimental results and to Eq. (4), there exists an optimal value of the fiber content. In particular, the peak of the mechanical performances is achieved in FRI-2, where the content of bio-fibers is QF = 56 g/dm^3. Further increment

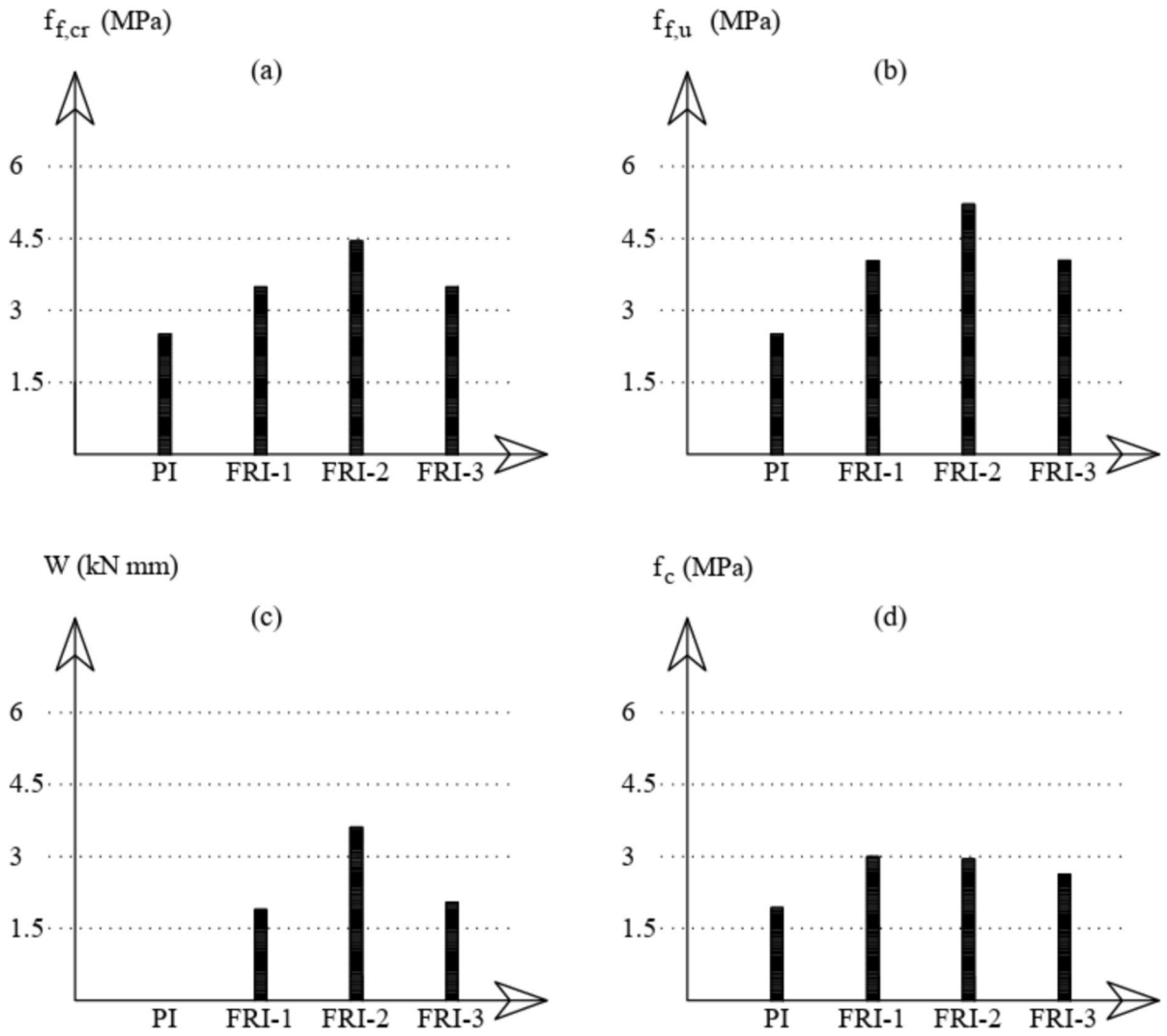

Fig. 7 Mechanical performances measured in the experimental campaign: (**a**) flexural strength at cracking (when $P = P_{cr}$ in Eq. (1)); (**b**) flexural strength at peak (when $P = P_u$ in Eq. (1)); (**c**) average value of the work (or energy) released during the deflection-hardening; and (**d**) average value of compressive strength

of QF, as in FRI-3, produces a decrement of all the mechanical performances.

As a possible explanation, this behavior may be attributed to the bond between the matrix (i.e. water) and the reinforcing elements (i.e., bio-fibers). When the quantity of fibers exceeds a certain threshold, it can cause the reduction of the matrix area surrounding the fibers. This situation, in turn, leads to a decrement of the bond strength between matrix and reinforcement, and therefore to a premature failure of FRI under compression and bending actions.

These results are also consistent with those measured by various researchers in fiber-reinforced concrete (FRC), in which every fiber content has a threshold (i.e., a maximum). Generally, a quadratic function, like Eq. (4), can be used to predict the mechanical performances of FRC from the content of fibers [22].

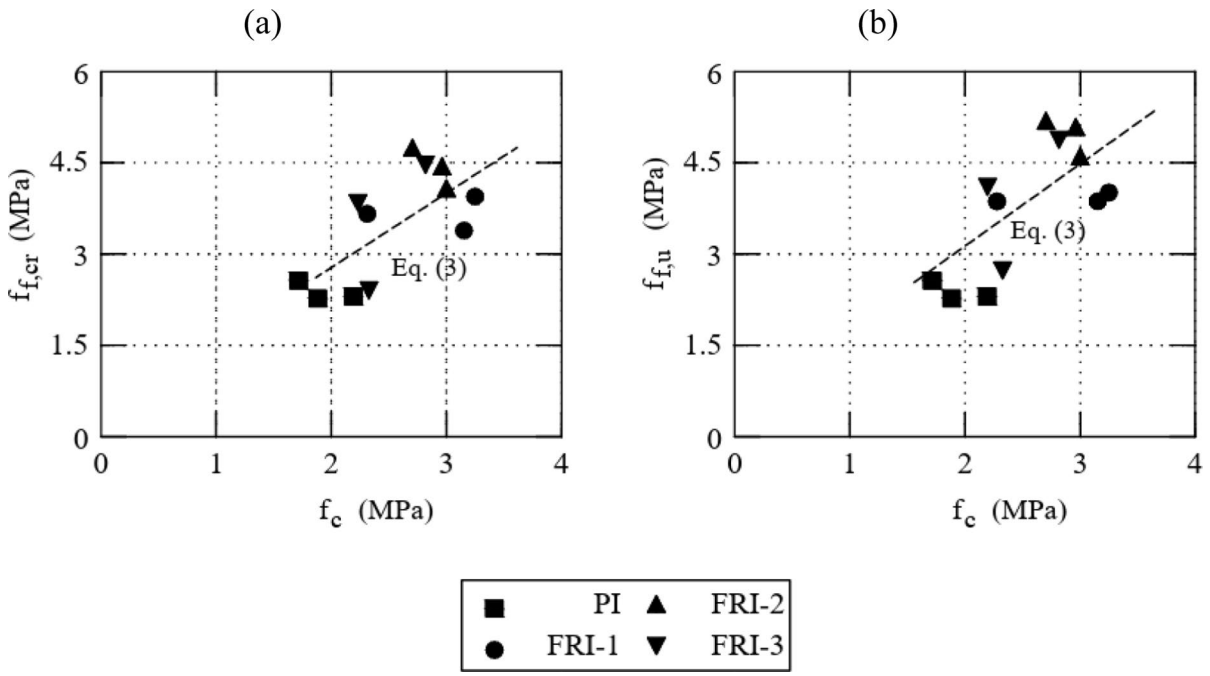

Fig. 8 Linear regression analyses (**a**) between $f_{f,cr}$ and f_c, and (**b**) between $f_{f,u}$ and f_c

Table 5 Values of the parameters a in Eq. (3) and of the coefficient of determination R^2

Strength	a	R^2
$f_{f,cr}$	1.3602	0.9693
$f_{f,u}$	1.5137	0.9636

5 Conclusion

The mechanical properties of FRI, measured with three-point bending and uniaxial compression tests, were examined in this study. Based on test results and the analysis of experimental data, the following conclusions can be made:

- In bending, the bearing capacity of plain ice drops dramatically after reaching the peak of stress, and a brittle failure occurs in presence of a single crack. Conversely, in FRI, more than one crack appears as the bending moment increases, and the bearing capacity increases as well after cracking. Due to the presence of a deflection hardening, FRI behaves in a more ductile manner than plain ice.
- In general, the mechanical properties of FRI improve due to the presence of fibers, and surpasses those of unreinforced ice. Test results indicate that the ultimate flexural strength of FRI can be twice than that of plain ice. Moreover, flexural strength is in direct proportion to the compressive strength.
- However, the mechanical properties of FRI are fiber-content sensitive. Indeed, they do not increase monotonically with the quantity of fibers. In other words, there exists an optimal content of fibers which guarantees the maximum performances. In the present case, the optimal value is reached in FRI-2, containing 56 g/dm^{3}of pine needles.

Finally, as ice is a temperature sensitive material, the effect of temperature on the strength and toughness of FRI will be investigated in the next phase of this study. Indeed, these research activities will help to define the potential of ice structures in terms of span, load, and functional versatility, paving the way for innovative applications in extreme environments.

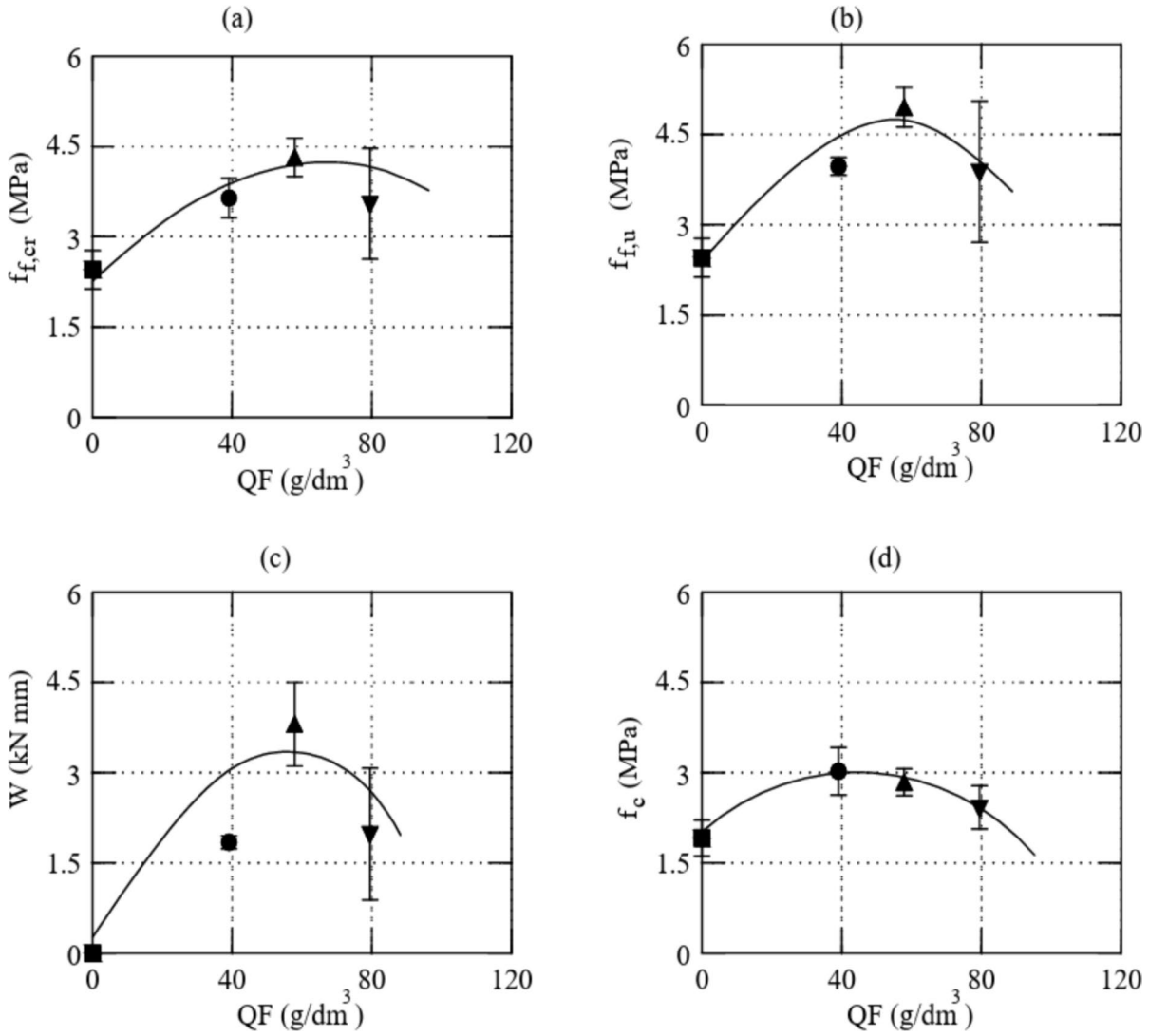

Fig. 9 Quadratic regression of $f_{f,cr}$, $f_{f,u}$, W, and f_c, with respect to the quantity of fibers QF

Table 6 Values of the parameters α, β, and γ in Eq. (4)

Mechanical performance	α	β	γ
$f_{f,cr}$	− 0.0005 MPa / (g/dm^3)^2	0.058 MPa / (g/dm^3)	2.4525 MPa
$f_{f,u}$	− 0.0007 MPa / (g/dm^3)^2	0.0774 MPa / (g/dm^3)	2.4319 MPa
W	− 0.0009 kN mm / (g/dm^3)^2	0.1012 kN mm / (g/dm^3)	− 0.098 kN mm
f_c	− 0.0005 MPa/ (g/dm^3)^2	0.0467 MPa / (g/dm^3)	1.917 MPa

Acknowledgements The present study has been developed within the National project AID-STRU—AgeIng and Degradation in the performances of STRUctures: model- and data-driven tools embedded in digital-twins (PRIN 2022). This study was also carried out within the Spoke 7 of the MOST—Sustainable Mobility National Research Center and received funding from the European Union Next-GenerationEU (PIANO NAZIONALE DI RIPRESA E RESILIENZA (PNRR)—MISSIONE 4 COMPONENTE 2, INVESTIMENTO 1.4—D.D. 1033 17/06/2022, CN00000023). This manuscript reflects only the authors' views and opinions. Neither the European Union nor the European Commission can be considered responsible for them.

Funding Open access funding provided by Politecnico di Torino within the CRUI-CARE Agreement.

References

1. Zhang Y (2016) Perspective of China's participation in polar development and governance. J Qingdao Univ Sci Technol (Soc Sci Ed) 32:75–78
2. Timco GW (ed) (1989) International association for hydraulic research (IAHR) Working group on ice forces–4th State-of-the-art report. US Army cold regions research and engineering laboratory special report 89–5, p 385
3. Vasiliev NK (1993) On development of fiber-ice-composites. Cold Reg Sci Technol 21:195–199. https://doi.org/10.1016/0165-232X(93)90007-U
4. Li JH, Wei Z, Wu C (2015) Preparation and properties of novel building materials at low temperature. Materials Design 65:329–336. https://doi.org/10.1016/j.matdes.2014.10.040
5. Barrette PD (2015) A review of guidelines on ice roads in Canada: determination of bearing capacity. In: Conference of the transportation association of Canada (TAC), Charlottetown, 19–20 September 2015, p 1–17 (available online at http://conf.tac-atc.ca/english/annualconference/tac2015/s24/barrette.pdf)
6. Vasiliev NK, Pronk ADC, Shatalina IN, Janssen FHME, Houben RWG (2015) A review on the development of reinforced ice for use as a building material in cold regions. Cold Reg Sci Technol 115:56–63. https://doi.org/10.1016/j.coldregions.2015.03.006
7. Marthinsen A (1986) Ice used as a permanent construction material. In: Proceedings of 5th international conference on offshore mechanics and arctic engineering (OMAE), Tokyo, Japan, ASME, vol IV, p 120–32
8. Glockner PG (1988) Reinforced ice and ice domes: opportunities for the North. Int J Space Struct 3(2):84–102. https://doi.org/10.1177/026635118800300203
9. Makkonen L (1994) Ice and construction. Technical Research Centre of Finland, Espoo
10. Haynes F, Martinson CR (1989) Ice reinforced with geogrid. In: Proceedings of 8th international conference on offshore mechanics and arctic engineering (OMAE), The Hague, Netherlands, ASME, vol IV, p 179–85
11. Nixon WA, Smith RA (1987) The fracture toughness of some wood-ice composites. Cold Reg Sci Technol 14:139–145. https://doi.org/10.1016/0165-232X(87)90029-2
12. Coble RL, Kingery WD (1962) Ice reinforcement. In: Kingery WD (ed) Proceedings of ice and snow, MIT Press, p 130–48
13. Tabassum S (2017) Study of mechanical properties of cellulose-reinforce ice. Aalto University, Espoo https://urn.fi/URN:NBN:fi:aalto-201705114710
14. Weber LJ, Nixon WA (1997) Fatigue of freshwater ice. Cold Reg Sci Technol. https://doi.org/10.1016/S0165-232X(97)00014-1
15. Kuehn GA, Nixon WA (1988) Reinforced ice: mechanical properties and cost analysis for its use in platforms and roads. In: Proceedings of 7th international conference on offshore mechanics and arctic engineering (OMAE), Houston, Texas, vol IV, p 193–200
16. Yue W, Xiaonan L, Xiuming L, Pron A (2020) The property of fiber reinforced ice under uniaxial compression. Mater Struct. https://doi.org/10.1617/s11527-020-01463-2
17. Farjon A (2005) Pines. In: Drawings and descriptions of the genus Pinus. Brill, Architecture, 2nd edn, p 235, ISBN-13: 978–9004139169
18. Fantilli AP, Dehkordi FM (2021) Two–stage cementitious composites containing recycled steel fibers. ACI Mater J 119(2):197–206
19. UNI EN 196-1 (2005) Methods of testing cement–Part 1: determination of strength. European Committee for Standardization, Brussels
20. Fantilli AP, Frigo B, Dehkordi FM (2022) Relationship between flexural strength and compressive strength in concrete and ice. In: Current perspectives and new directions in mechanics, modelling and design of structural systems, 1st edn. CRC Press, p 6, ISBN 9781003348443
21. Fantilli AP, Dehkordi FM (2021) Tailoring HPFRC with materials from end of life tires - HPFRC ottenuti con materiali provenienti dagli pneumatici a fine vita. In: Costruire in calcestruzzo: realizzazioni, ricerca, attualità e prospettive. Proceedings of Italian concrete days 2020, p 743–752 (in Italian)
22. Zhao C, Wang Z, Zhu Z, Guo Q, Wu X, Zhao R (2023) Research on different types of fiber reinforced concrete in recent years: an overview. Constr Build Mater 365:130075. https://doi.org/10.1016/j.conbuildmat.2022.130075